On Bending of Multi-Equi-Cell Plate

On Bending of Multi-Equi-Cell Plate

Sumio G. Nomachi*

Abstract

Bending of a orthotropic plate which is built up in multi-equi-cell profile by many long rectangular strips, is considered here. Making use of Displacement-Shear Equations concerning folded plate theory, we can write equilibrium of forces at a longitudinal joint, in four finite difference equations with respect to three components of displacement and rotation, and an analitical method for solving those finite difference equations by means of finite Fourier transforms based on finite integration, is discussed. As numerical examples, the case when four sides are simply supported and the case when two edges of multi-cell profile are free and remaining two sides are simple supported, are presented.

1. Introduction

A few studies on multi-cell bridge structure can so far be found[1)2)3)], they might, however, be far from so to speak "Multi-Cell Plate", because number of the cell is too short to be called so. While the recent studies on multiple folded plate structures have made remarkable progress relating to the computor technique either in elasticity theory[4)] or ordinary folded plate theory[5)6)]. A. C. Scordelis and his colleague members settled the elasticity theory program, written for the IBM-7094, which was capable of analyzing simple span structures with up to 150 plates and 100 longitudinal joints, and the program used a harmonic analisis in which as many as 100 nonzero terms of the appropriate Fourier series might be selected to represent each load on the structure. As for the ordinary folded plate theory, quite a few programs have already been fixed and many valuable numerical examples

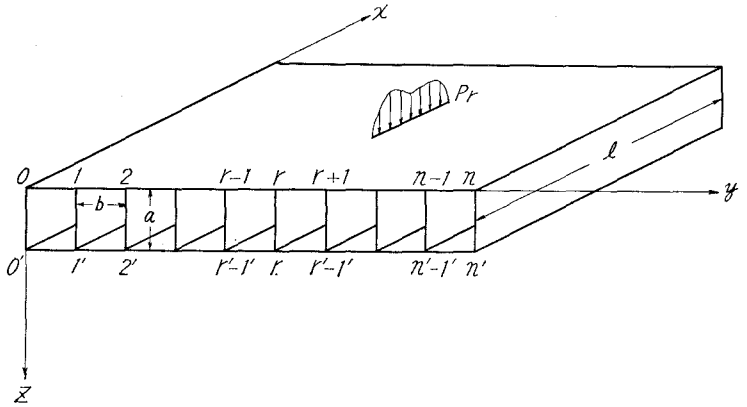

Fig. 1.

* Member of Japan Society of Civil Engineers.
Muroran Institute of Technology, Muroran-City.

have been presented. It may therefore be true that there is no new on the view point of numerical calculation about the multi-cell plate with simple pan, but it may still be important to seek an analitical way for the solution, because we may not only check the differential equation which is supposed to approximately express the bending of multi-equi-cell plate, but also be able to simplify the program for the computor by taking the analitical result into account.

The presenting paper deals with the simple span n-cell plate as shown in Fig. 1, the upper and lower longitudinal joints of which are numbered by r and R, and the three components of displacement u, v, w with subscription r denote the components at the r-th joint in the x, y, z directions.

2. Displacement-Shear Equation of Long Rectangular Strip r, $r+1$

Co-ordinates s and x are located on the rectangular strip r, $r+1$ as shown in Fig. 2, p_s and p_x denote the normal fo rces in the s and x directions, and let q be the shearing force, then we have the following equations:

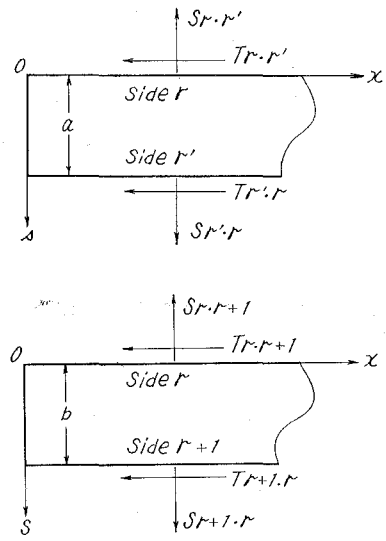

Fig. 2.

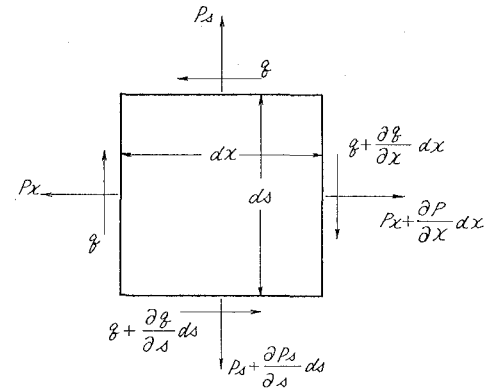

Fig. 3.

$$\frac{\partial p_s}{\partial s}+\frac{\partial q}{\partial x}=0 \tag{1}$$

$$\frac{\partial p_x}{\partial x}+\frac{\partial q}{\partial s}=0 \tag{2}$$

$$p_x=\frac{Et}{1-\nu^2}\left(u'+\nu\frac{\partial v}{\partial s}\right), \tag{3}$$

$$p_s=\frac{Et}{1-\nu^2}\left(\frac{\partial v}{\partial s}+\nu u'\right), \tag{4}$$

$$q = Gt\left(\frac{\partial u}{\partial s} + v'\right) \tag{5}$$

where E, G: elastic modulus, shear modulus,
t: thickness,

and

$$u' = \frac{\partial u}{\partial x}, \quad v' = \frac{\partial v}{\partial y}.$$

The variation of u is assumed to be linear about s like in the folded plate theory, and let us introduce the normal strain in the s direction as the linear variation of s which may be appropriate for the long strip, in order to take the effect of Poisson's ratio on the stresses into account.
Thus

$$u = u_r(1-s/b)+u_{r+1}s/b \tag{7}$$

$$\frac{\partial v}{\partial s} = e_r(1-s/b)+e_{r+1}s/b \tag{8}$$

which together with (4) yield

$$p_s)_{s=0} = S_{r,r+1} = \frac{Et}{1-\nu^2}(e_r+\nu u_r') \tag{9}$$

$$p_s)_{s=b} = S_{r+1,r} = \frac{Et}{1-\nu^2}(e_{r+1}+\nu u_{r+1}') \tag{10}$$

and integration of (8) from 0 to b with respect to s is found that

$$2\Delta v_r = b(e_r+e_{r+1}) \tag{11}$$

Since the strip is long, it can be assumed that

$$\int_0^b v\,dx = \frac{b}{2}(v_{r+1}+v_r) \tag{12}$$

and the above defnite integration is also carried out from (8):

$$\int_0^b v\,dx = \frac{b^2}{6}(2e_r+e_{r+1}) + bv_r, \tag{13}$$

which and (12) finally give

$$\frac{1}{2}\Delta v_r = \frac{b}{6}(2e_r+e_{r+1}). \tag{14}$$

The assumption we take in (12) is that the quantity of $e_{r+1}-e_r$ is small enough to neglect in comparsion with $e_{r+1}+e_r$. Writing p_x in (2) by (7) and (8), and integrating it with respect to s, we get

$$q = T_{r\cdot r+1} - \frac{Et}{1-\nu^2}\left\{(u_r'' + e_r')\left(s - \frac{s^2}{2b}\right) + (u_{r+1}'' + e_{r+1}')\frac{s^2}{2b}\right\} \tag{15}$$

from which

$$T_{r\cdot r+1} + T_{r+1\cdot r} = \frac{Et}{2(1-\nu^2)}(u_r + u_{r+1} + e_r + e_{r+1}) \tag{16}$$

because $q = T_{r\cdot r+1}$, $q = -T_{r+1\cdot r}$ for $s = 0, b$.

After substituting (15) into (1) and integrating it again from 0 to b with respect to s, the displacement shear equation takes the following form;

$$T_{r\cdot r+1}' = \frac{N}{6}(2u_r''' + u_{r+1}''') + \frac{\nu N}{6}(2e_r'' + e_{r+1}'') + (S_{r\cdot r+1} - S_{r+1\cdot r})/b\,, \tag{17}$$

which and (16) lead to

$$T_{r+1\cdot r}' = \frac{N}{6}(2u_{r+1}''' + u_r''') + \frac{\nu N}{6}(2e_{r+1}'' + e_r'') + (S_{r+1\cdot r} - S_{r\cdot r+1})/b\,, \tag{18}$$

The 2nd terms on the right sides of (17) and (18) can be replaced by v with the consideration of (14), and they are rewritten as

$$T_{r\cdot r+1}' = \frac{N}{6}(2u_r''' + u_{r+1}''') + \frac{\nu N}{2b}(v_{r+1}'' - v_r'') + (S_{r\cdot r+1} - S_{r+1\cdot r})/b\,, \tag{19}$$

$$T_{r+1\cdot r}' = \frac{N}{6}(2u_{r+1}''' + u_r''') + \frac{\nu N}{2b}(v_{r+1}'' - v_r'') + (S_{r+1\cdot r} - S_{r\cdot r+1})/b\,. \tag{20}$$

where $N = Ebt/(1-\nu^2)$

3. Displacement v and Bending Moment at the Longitudinal Joint

Differentiating (5) with respect to x and then integrating with respect to s from 0 to b, we finally come to the result by negleting those smaller terms, as follows:

$$\frac{Gbt}{2}(v_{r+1} + v_r) = -Gt\Delta u_r + S_{r\cdot r+1} - S_{r+1\cdot r} \tag{21}$$

and for the diaphragm member r R,

$$\frac{Gat}{2}(w_r + w_R) = Gt(u_r - u_R) + S_{r\cdot R} - S_{R\cdot r}\,. \tag{22}$$

Besides those formulas, the bending moments which take place at the joint to prevent the cells from the deformation and the shearing forces following them, must be formulated. For this purpose the slope deflection equation is to be used.

$$M_{r\cdot r+1} = 2K(2\theta_r + \theta_{r+1} - 3\Delta w_r/b) \tag{23}$$

$$M_{r+1\cdot r}=2K(2\theta_{r+1}+\theta_r-3\Delta w_r/b) \tag{24}$$

$$M_{r\cdot R}=2K_I\left\{2\theta_r+\theta_R-3(v_r-v_R)/a\right\} \tag{25}$$

$$bX_{r\cdot r+1}=-6K(\theta_r+\theta_{r+1}-2\Delta w_r/b) \tag{26}$$

$$aX_{r\cdot R}=-6K_I\left\{\theta_r+\theta_R-2(v_r-v_R)/a\right\} \tag{27}$$

$$X_{r\cdot r+1}=X_{r+1\cdot r}$$

where $M_{r\cdot r+1}$: bending moment about the joint r in the upper member r, $r+1$,
$X_{r\cdot r+1}$: shearing force at the joint r caused by both edge moments of the member r, $r+1$
$\Delta w_r=w_{r+1}-w_r$.

4. Equilibrium of Forces at the Joint r

It is easily seen from Fig. 4 that the four equilibrium equations should be written as follows:

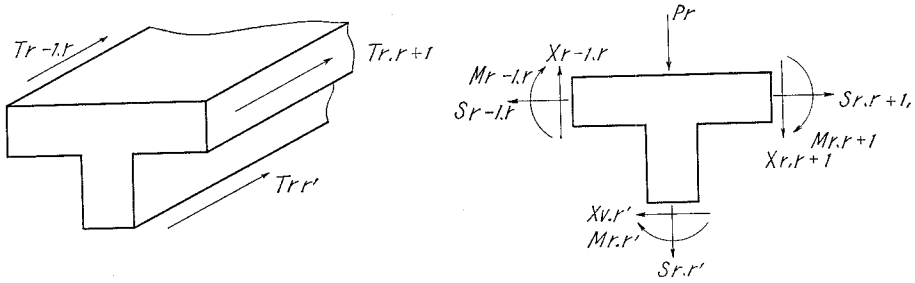

Fig. 4. Forces around Joint r.

$$S_{r\cdot r+1}-S_{r\cdot r-1}-X_{r\cdot R}=0 \tag{29}$$

$$S_{r\cdot R}+P_r+X_{r\cdot r+1}-X_{r\cdot r-1}=0 \tag{30}$$

$$T_{r\cdot r+1}+T_{r\cdot r-1}+T_{r\cdot R}=0 \tag{31}$$

$$M_{r\cdot r+1}+M_{r\cdot r-1}+M_{r\cdot R}=0 \tag{32}$$

into which the substitution of R for r and r for R, yields equilibrium of forces at the lower joint R.

Let S_r be the mean value of $S_{r\cdot r+1}$ and $S_{r\cdot r-1}$, then

$$S_{r\cdot r+1}=S_r+\frac{1}{2}X_{r\cdot R},\qquad S_{r\cdot r-1}=S_r-\frac{1}{2}X_{r\cdot R} \tag{33}$$

which will make the forthcoming expressions simple.

For an instance,

$$S_{r\cdot r+1}-S_{r+1\cdot r}+S_{r\cdot r-1}-S_{r-1\cdot r}=-\Delta^2 S_{r-1}+\frac{1}{2}\bar{\Delta}X_{r\cdot R} \tag{34}$$

$$S_{r\cdot r+1}+S_{r+1\cdot r}+S_{r\cdot r-1}+S_{r-1\cdot r}=\Delta^2 S_{r-1}+4S_r-\frac{1}{2}\bar{\Delta}X_{R\cdot r} \tag{35}$$

where $\bar{\Delta}X_{r\cdot R}=X_{r+1\cdot R+1}-X_{r-1\cdot R-1}$.

We find from (30), that

$$S_{r\cdot R}=\frac{6K}{b}(\bar{\Delta}\theta_r-2\Delta^2 w_{r-1}/b)-P_r\,. \tag{36}$$

The substitution of the displacement shear equations into (31) yields

$$\frac{N}{6}(\Delta^2 u'''_{r-1}+6u'''_r)+\frac{N_1}{6}(2u'''_r+u'''_R)+\frac{\nu N}{2b}\bar{\Delta}v''_r$$
$$+(S_{r\cdot r+1}-S_{r+1\cdot r}+S_{r\cdot r-1}-S_{r-1\cdot r})/b+(S_{r\cdot R}-S_{R\cdot r})=0$$

which by the aid of (21), is rewritten in the followign form

$$\frac{N}{6}(\Delta^2 u'''_{r-1}+6u'''_r)+\frac{N_1}{6}(2u'''_r+v'''_R)+\frac{\nu N}{2b}\bar{\Delta}v_r$$
$$+\frac{Gt}{2}\bar{\Delta}v_r+\frac{Gt}{b}\Delta^2 u_{r-1}+(S_{r\cdot R}-S_{R\cdot r})/a=0\,. \tag{37}$$

Similary the slope deflection equations transform (32) into

$$2K(\Delta^2\theta_{r-1}+6\theta_r)-6K\bar{\Delta}w_r/b$$
$$+2K_1(2\theta_r+\theta_R)-\frac{6K_1}{a}(v_r-v_R)=0\,. \tag{38}$$

Replacing the left side of (34) by (21), we get

$$Gbt\bar{\Delta}v_r+2Gt\Delta^2 u_{r-1}=-2\Delta^2 S_{r-1}+\bar{\Delta}X_{r\cdot R}\,, \tag{39}$$

and putting (9), (10) into the left side of (35), we find

$$2N\bar{\Delta}v_r+Nb(\Delta^2 u'_{r-1}+4u'_r)=4b^2 S_r+b^2\Delta^2 S_{r-1}-\frac{1}{2}b^2\bar{\Delta}X_{r\cdot R} \tag{40}$$

where

$$\bar{\Delta}X_{r\cdot R}=-6K_1(\bar{\Delta}\theta_r+\bar{\Delta}\theta_R-2\bar{\Delta}v_r/a+2\bar{\Delta}v_R/a)\,.$$

The diaphragm member may play a part like the web in the I-beam, so that the effect of the bending on the deflection w is more major than that of the shearing. The equation (22) can, therefore, be rewritten as

$$w'_r=(u_r-u_R)/a\,, \tag{41}$$

which is observed that the difference of w between r and R is neglected.

Substitutions of r, R for R, r in (37), (38) excluding the last term (v_r-v_R), (39) and (40) with the consideration of $X_{r\cdot R}+X_{R\cdot r}=0$, lead to another set of equations for the longitudinal joint R. So doing, we have nine finite difference equations for nine unkown values u_r, u_R, v_r, v_R, w_r, S_r, S_R, θ_r, θ_R.

5. Boundary Conditions

Three component strips meet with one another at the joints r and R, but Two component strips make the edge joint where $r=0$, $R=0$, or $r=n$, $R=n$, so that the equilibriums of shearing forces and end moments are expressed by

$$T_{0\cdot1}+T_{0\cdot R}=0\,,\qquad M_{0\cdot1}+M_{0\cdot R}=0\,,$$

which yield

$$\frac{(N+N_0)}{3}u_0'''+\frac{N}{6}u_1'''+\frac{N_0}{6}u_R'''+\frac{\nu N}{2b}(v_1''-v_0'')$$
$$+\frac{Gt}{2}(v_1''+v_0'')+\frac{Gt}{b}(u_1'-u_0')+(S_{0\cdot R}-S_{R\cdot0})/a=0\,, \tag{42}$$

$$2K(2\theta_0+\theta_1)+2K_0(2\theta_0+\theta_R)-6K(w_1-w_0)/b$$
$$-6K_0(v_0-v_R)/a=M_0\,, \tag{43}$$

and

$$S_{0\cdot1}-Y_0=X_{0\cdot R} \tag{44}$$

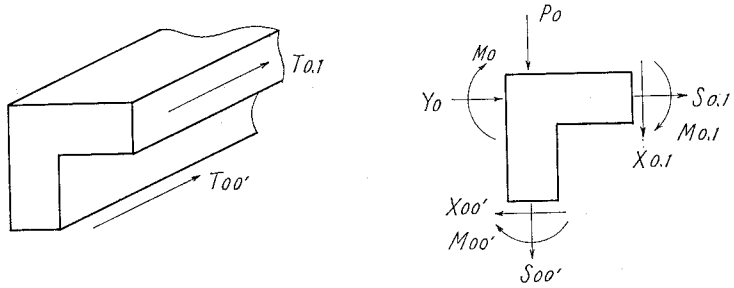

Fig. 5. Forces around Joint 0.

where Y_0 denotes a horizontal force acting at the upper joint zero, M_0 an external moment at the same joint,

K_0 denotes the flexural rigidity of the diaphragm for $r=0$,

R shows the joint zero at the bottom flange,

$N_0=Ebt/(1-\nu^2)$,

$$X_0=-\frac{6K_0}{a}\left\{\theta_0+\theta_R-2(v_0-v_R)/a\right\}\,, \tag{45}$$

From (33) as well as (27), we find for $r=0$

$$S_{0\cdot1}-S_0=-\frac{3K_1}{a}\left\{\theta_0+\theta_R-2(v_0-v_R)/a\right\}$$

which together with (44) and (45) leads, if K_0 is $K_1/2$, to the relation

$$S_0=Y_0\,. \tag{46}$$

Substitution of n for the subscription 0 in the above expressions furnishes, by letting the subscription R denote the bottom joint n, the boundary conditions for the top joint n. For the bottom joint 0, the boundary conditions are written in the forms

$$\frac{(N'+N_0)}{3}u'''_R+\frac{N'}{6}u'''_{R+1}+\frac{N_0}{6}u'''_0+\frac{\nu N}{2b}(v''_{R+1}-v''_R)$$
$$+\frac{Gt'}{2}(v''_{R+1}+v''_R)+\frac{Gt'}{b}(u'_{R+1}-u'_R)-(S_{0\cdot R}-S_{R\cdot 0})/a=0\,, \tag{47}$$

$$2K'(2\theta_R+\theta_{R+1})+2K_0(2\theta_R+\theta_0)-6K'(w_{R+1}-w_R)/b$$
$$-6K_0(v_0-v_R)/a=0\,, \tag{48}$$

$$a(S_R-Y_R)-3(K_1-K_0)\left\{\theta_0+\theta_R-2(v_0-v_R)/a\right\}=-M_n\,, \tag{49}$$

where $N'=Et'b/(1-\nu^2)$, K' denotes the flexural regidity of the bottom flange, t' is thickness of the bottom flange, R denotes the bottom joint zero, Y_R stands for the horizontal force at the bottom joint zero.

When the subscriptions 0, $R+1$ are substituted by n, $R-1$ in the equations (47), (48), and (49), these equations become by letting R represent the bottom joint n, the boundary conditions which may be satisfied at the prescribed joint.

6. Case when the Profile is Symmetrical with Respect to Center Lines Parallel to x and y Axes

A. Equations and Boundary Conditions.

In this case, it is readily seen that

$$u_r+u_R=0\,,\quad v_r+v_R=0\,,\quad \theta_r-\theta_R=0\,,$$
$$S_r+S_R=0\,,\quad w_r=2u_r/a\,,$$

and the equations (37)~(40) may be written

$$\frac{Na}{12}(\Delta^2w''''_{r-1}+6w''''_r)+\frac{aN_1}{12}w''''_r+\frac{1}{2}\left(\frac{N\nu}{b}+Gt\right)\bar{\Delta}v''_r$$
$$+\frac{aGt}{2b}\Delta^2w''_{r-1}+\frac{12K}{b}(\bar{\Delta}\theta_r-2\Delta^2w_{r-1}/b)/a-P_r/a=0\,, \tag{50}$$

$$2K(\Delta^2\theta_r+6\theta_r)+2K_1\theta_r-6K\bar{\Delta}w_r/b-12K_1v_r/a=0\,, \tag{51}$$

$$\frac{1}{2}Gbt\bar{\Delta}v''_r-6K_1\bar{\Delta}v_r/a+3K_1\bar{\Delta}\theta_r+\frac{Gat}{2}\Delta^2w''_{r-1}=-\Delta^2S_r \tag{52}$$

$$(2N/b^2+6K_1/a)\bar{\Delta}v_r+Na\nu(\Delta^2w''_{r-1}+4w''_r)/2b-3K_1\bar{\Delta}\theta_r$$
$$=\Delta^2S_{r-1}+4S_r\,, \tag{53}$$

which are the fundamental finite difference and differential equations for the case of same flange thickness.

The bondary conditions corresponding to the above, may be written from (42), (43), and (46), as follows

$$a\left(N+\frac{N_0}{2}\right)w_0''''/6+Nw_1''''/12+\nu N(v_1''-v_0'')/2b$$
$$+\frac{Gt}{2}(v_1''+v_0'')+Gta(w_1''-w_0'')/2b=2X_{0\cdot1}/a+P_0/a\,, \tag{54}$$

$$2K(2\theta_0+\theta_1)+6K_0\theta_0-6K(w_1-w_0)/b-12K_0v_0/a=-M_0 \tag{55}$$

$$S_0=Y_0$$

and another set of boundary conditions for $r=n$, are as follows

$$a\left(N+\frac{N_0}{2}\right)w_n''''/6+aNw_{n-1}''''/12+\nu N(v_n''-v_{n-1}'')/2b$$
$$+\frac{1}{2}Gt(v_n''+v_{n-1}'')+Gta(w_n''-w_{n-1}'')/2b=(2X_{n-1\cdot n}+P_n)/a\,, \tag{56}$$

$$2K(2\theta_n+\theta_{n-1})+6K_0\theta_n-6K(w_n-w_{n-1})/b-12K_0v_n/a=-M_n\,. \tag{57}$$

$$S_n=Y_n\,.$$

B. Finite Fourier Transforms of v, w, θ, and S concerning Fourier Integral and Finite Integration with Respect to x and r respectively.

As stated before the structure is simply supported in the x direction, and if the both ends are closed by the rigid diaphragms in the y direction, the following expressions hold:

$$v_r=\theta_r=w_r=w_r=S_r=0\,, \qquad \text{for} \quad x=0,\ 1\,,$$

which shows that v_r, θ_r, w_r, and S_r may be conveniently described by the finite sine transform with respect to x, while the finite difference part in the equations (50), (53) may be analitically solved by means of finite Fourier transforms concerning the finite integration[7)8)]. It accordingly follows that

$$\left.\begin{aligned} v_r &= \frac{4}{nl}\sum_{m=1}^{\infty}\sum_{i=0}^{n}V_{im}\sin\frac{m\pi x}{l}\cos\frac{i\pi r}{n}\\ \theta_r &= \frac{4}{nl}\sum_{m=1}^{\infty}\sum_{i=0}^{n}\Theta_{im}\sin\frac{m\pi x}{l}\cos\frac{i\pi r}{n}\\ w_r &= \frac{4}{nl}\sum_{m=1}^{\infty}\sum_{i=0}^{n}W_{im}\sin\frac{m\pi x}{l}\sin\frac{i\pi r}{n}\\ S_r &= \frac{4}{nl}\sum_{m=1}^{\infty}\sum_{i=1}^{n}H_{im}\sin\frac{m\pi x}{l}\sin\frac{i\pi r}{n} \end{aligned}\right\} \tag{58}$$

where i, m are integers,

in which

$$
\begin{aligned}
V_{0m} &= \frac{1}{4}\int_0^l \sin\frac{m\pi x}{l}dx\left\{v_0+v_n+2\sum_{r=1}^{n-1}v_r\right\}\\
V_{nm} &= \frac{1}{4}\int_0^l \sin\frac{m\pi x}{l}dx\left\{v_0+(-1)^n v_n+2\sum_{r=1}^{n-1}v_r(-1)^r\right\} \qquad (60)\\
V_{im} &= \frac{1}{2}\int_0^l \sin\frac{m\pi x}{l}dx\left\{v_0+(-1)^i v_n+2\sum_{r=1}^{n-1}v_r\cos\frac{i\pi r}{n}\right\}\\
\Theta_{0m} &= \frac{1}{4}\int_0^l \sin\frac{m\pi x}{l}dx\left\{\theta_0+\theta_n+2\sum_{r=1}^{n-1}\theta_r\right\}\\
\Theta_{nm} &= \frac{1}{4}\int_0^l \sin\frac{m\pi x}{l}dx\left\{\theta_0+(-1)^n\theta_n+2\sum_{r=1}^{n-1}\theta_r(-1)^r\right\} \qquad (60)\\
\Theta_{im} &= \frac{1}{2}\int_0^l \sin\frac{m\pi x}{l}dx\left\{\theta_0+(-1)^i\theta_n+2\sum_{r=1}^{n-1}\theta_r\cos\frac{i\pi r}{n}\right\}
\end{aligned}
$$

$$
W_{im}=\int_0^l \sin\frac{m\pi x}{l}dx\sum_{r=1}^{n-1}w_r\sin\frac{i\pi r}{n} \qquad (61)
$$

$$
H_{im}=\int_0^l \sin\frac{m\pi x}{l}dx\sum_{r=1}^{n-1}S_r\sin\frac{i\pi r}{n} \qquad (62)
$$

Multiplying (50), (52), (53) by $\sin m\pi x/l\cdot\sin i\pi r/n$ and integrating from 0 to 1 with respect to x as well as carrying on the finite integration between 1 and $n-1$ with respect to r, we find that

$$
\begin{aligned}
&W_{im}\left[(m\pi/l)^4\left\{Na(6-D_i)+N_1a\right\}/12+D_i(1-\nu)(Na/b^2)(m\pi/l)^2/4+24(K/a)(D_i/b^2)\right]\\
&\quad+V_{im}\sin i\pi/n\cdot N(m\pi/l)(1+\nu)/(2b)-\Theta_{im}\sin i\pi/n\cdot 24K/(ab)\\
&\quad=P_{im}/a+\sin i\pi/n\left\{W_{nm}(-1)^i-W_{0m}\right\}\left\{(m\pi/l)Na/12-24K/(ab^2)\right.\\
&\quad\left.-(m\pi/l)^2(1-\nu)Na/(2b^2)\right\}, \qquad (63)
\end{aligned}
$$

$$
\begin{aligned}
&V_{im}\sin i\pi/n\left\{(m\pi/l)^2Gbt+24K_1/a^2\right\}-\frac{12K_1}{a}\Theta_{im}\sin i\pi/n\\
&\quad+W_{im}D_i\frac{Gta}{2}\left(\frac{m\pi}{l}\right)^2-H_{im}D_i=-\frac{Gta}{2}\sin i\pi/n\left\{W_{nm}(-1)^i-W_{0m}\right\}\times\\
&\quad(m\pi/l)^2+\sin i\pi/n\left\{H_{nm}(-1)^i-H_{0m}\right\}, \qquad (64)
\end{aligned}
$$

$$
\begin{aligned}
&4V_{im}(N+6K_1b^2/a^2)\sin i\pi/n+W_{im}\frac{Nab\nu}{2}(4-D_i)(m\pi/l)^2\\
&\quad-12K\Theta_{im}(b^2/a)\sin i\pi/n-b^2(4-D_i)H_{im}\\
&\quad=\frac{Nab\nu}{2}\sin i\pi/n\left\{W_{nm}(-1)^i-W_{0m}\right\}(m\pi/l)^2-\sin i\pi/n\left\{H_{nm}(-1)^i-H_{0m}\right\} \qquad (65)
\end{aligned}
$$

where

$$D_i = 2(1-\cos i\pi/n),$$

$$W_{nm} = \int_0^l w_n \sin\frac{m\pi x}{l}\,dx \qquad W_{0m} = \int_0^l w_0 \sin\frac{m\pi x}{l}\,dx$$

$$H_{nm} = \int_0^l S_n \sin\frac{m\pi x}{l}\,dx \qquad H_{0m} = \int_0^l S_0 \sin\frac{m\pi x}{l}\,dx$$

And multiplying (51) by $\sin m\pi x/l \cdot \cos i\pi/n$ and doing the same procedure as above, we obtain

$$\begin{aligned}&\left\{2K(6-D_i)+6K_1\right\}\Theta_{im}-12K_1V_{im}/a-\frac{12K}{b}W_{im}\cdot\sin i\pi/n\\&=-M_{nm}(-1)^i-M_{0m}-3(2K_0-K_1)\left\{\theta_{nm}(-1)^i+\theta_{0m}-2v_{nm}(-1)^i/a\right.\\&\quad\left.-2v_{0m}/a\right\}+\frac{3K}{b}(4-D_i)\left\{W_{nm}(-1)^i-W_{0m}\right\},\end{aligned}\tag{66}$$

where

$$M_{nm} = \int_0^l M_n \sin\frac{m\pi x}{l}\,dx, \qquad M_{0m} = \int_0^l M_0 \sin\frac{m\pi x}{l}\,dx$$

$$\theta_{nm} = \int_0^l \theta_n \sin\frac{m\pi x}{l}\,dx, \qquad \theta_{0m} = \int_0^l \theta_0 \sin\frac{m\pi x}{l}\,dx$$

$$v_{nm} = \int_0^l v_n \sin\frac{m\pi x}{l}\,dx, \qquad v_{0m} = \int_0^l v_0 \sin\frac{m\pi x}{l}\,dx$$

Solving the equation (63), (66), we can determine V_{im}, W_{im}, and H_{im} and readily obtain w_r, S_r by virtue of the inversion formulas (58), but in order to get v_r, θ_r we need four more expressions standing for V_{0m}, V_{nm}, Θ_{0m} and Θ_{nm}.

We let, for this purpose, i be zero in (64) and (66), then

$$\begin{aligned}&V_{0m}\left\{Gbt(m\pi/l)^2+24K_1/a^2\right\}-12K_1\Theta_{0m}/a\\&\qquad=\frac{Gta}{2}(m\pi/l)^2(W_{nm}-W_{0m})+H_{nm}-H_{0m},\end{aligned}\tag{67}$$

$$\begin{aligned}&2\Theta_{0m}(6K+3K_1)-12K_1V_{0m}/a\\&\quad=-M_{nm}-M_{0m}-3(2K_0-K_1)\left\{\theta_{nm}+\theta_{0m}-2(v_{nm}+v_{0m})/a\right\}\\&\qquad\qquad+12K(W_{nm}-W_{0m})/b,\end{aligned}\tag{68}$$

which may furnish V_{0m} and Θ_{0m}: and let i be n, we have

$$\begin{aligned}&V_{nm}\left\{Gbt(m\pi/l)^2+24K_1/a^2\right\}-12K_1\Theta_{nm}/a\\&\qquad=\frac{Gta}{2}(m\pi/l)^2\left\{W_{nm}(-1)^n-W_{0m}\right\}+H_{nm}(-1)^n-H_{0m},\end{aligned}\tag{69}$$

$$2\Theta_{nm}(2K+3K_1)-12K_1V_{nm}/a=-M_{nm}(-1)^n-M_{0m}$$
$$-3(2K_0-K_1)\left[\theta_{nm}(-1)^n+\theta_{0m}-2\left\{V_{nm}(-1)^n+V_{0m}\right\}/a\right], \qquad (70)$$

from which V_{nm} and Θ_{nm} may be found. The unknown values W_{nm} and W_{0m} can be determined by the boundary conditions (54) and (56), while H_{nm} and H_{0m}, by (55) and (57). As for θ_{nm}, θ_{0m}, v_{nm} and v_{0m}, we must settle them as to satisfy

$$\left.\begin{aligned}\frac{nl}{4}v_{mn}&=\sum_{i=0}^{n}V_{im}(-1)^i, \qquad \frac{nl}{4}v_{0m}=\sum_{i=0}^{n}V_{im},\\ \frac{nl}{4}\theta_{nm}&=\sum_{i=0}^{n}\Theta_{im}(-1)^i, \qquad \frac{nl}{4}\theta_{0m}=\sum_{i=0}^{n}\Theta_{im}.\end{aligned}\right\} \qquad (71)$$

If the multicell plate is so made as $K_0=K/2$, and the loads only vertically act on the longitudinal joints in other words;

$$Y_0=Y_n=M_0=M_n=0,$$

the right sides of (68) and (70) become $12K(W_{nm}-W_{0m})$ and zero, respectively; and S_0 and S_n also, zero.

C. Numerical Examples

Let the flexural rigidity of the edge diaphragms K_0 be a half of K_1 that is of the other diaphragms, then the term of θ_{nm}, θ_{m0}, v_{nm}, v_{0m}, should be cancelled out in (66), (68), and (70). In so assuming, we are going to take two cases of the boundary conditions into account: the one is simply supported for $r=0$, n, and the other is free from any constraint for $r=0$, n.

(a) In case of simple span subjected a single concentrated load,

$$P_r=P \qquad \text{for} \quad x=f, \quad r=c,$$
$$P_r=0 \qquad \text{for} \quad x=f, \quad r=c,$$
$$W_{nm}=W_{0m}=0,$$

from which

$$P_{im}=P\sin\frac{m\pi f}{l}\sin\frac{i\pi c}{n}.$$

The coefficients are as follows

$$n=10, \quad a=b=10.0\text{ cm}, \quad =100.0\text{ cm},$$
$$f=l/2, \quad c=n/2,$$

of which σ_x, and deflection w are shown in Fig. 6, 7, and 8; and they are corresponding with

$$t=t_0=0.5\text{ cm}, \qquad E=2.1\times10\text{ kg/cm}^2, \quad \nu=0.3,$$
$$t=1.0\text{ cm}, \quad t_0=2.0\text{ cm}, \qquad E=2.1\times10\text{ kg/cm}^2, \quad \nu=0.15,$$
$$t=t_0=2.5\text{ cm}, \qquad E=2.1\times10\text{ kg/cm}^2, \quad \nu=0.15,$$

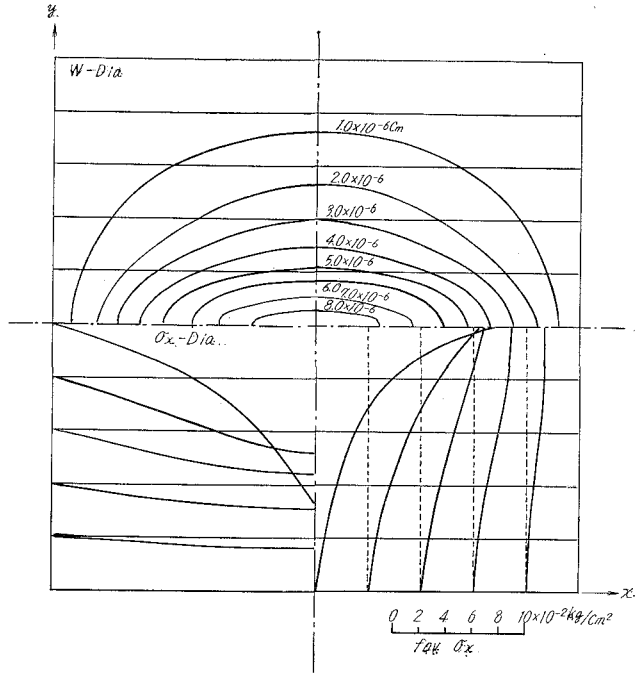

Fig. 6. W and σ_x Diagrams ($l=100$ cm, $a=b=10$ cm, $t=t_0=0.5$ cm, $E=2.1\times10^6$ kg/cm, $\nu=0.3$).

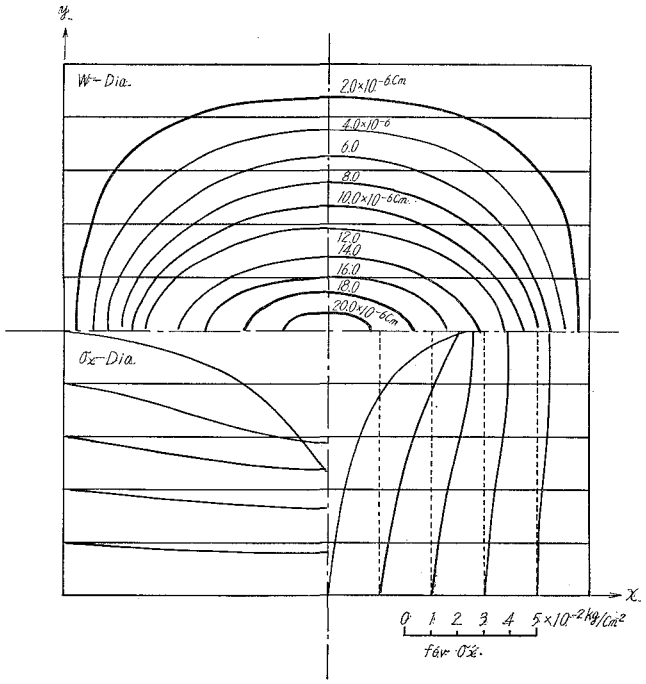

Fig. 7. W and σ_x Diagrams ($l=100$ cm, $a=b=10$ cm, $t=1.0$ cm, $t_0=2.0$ cm, $E=2.1\times10^5$ kg/cm, $\nu=0.3$).

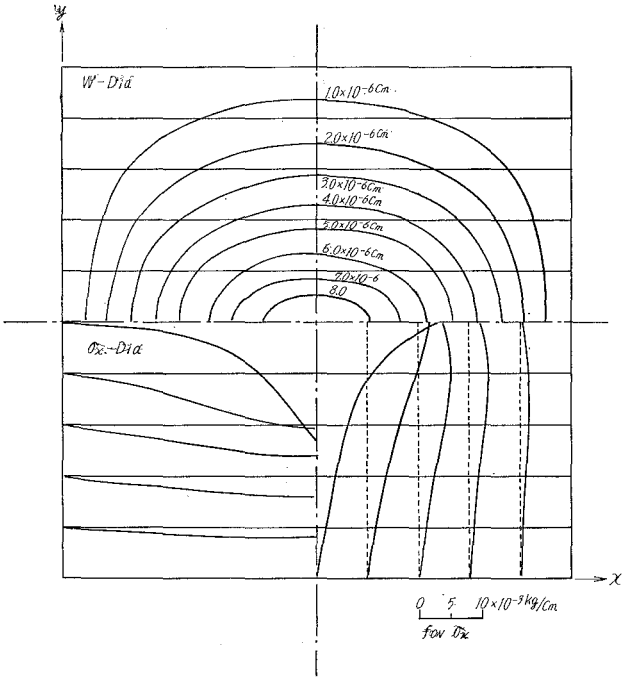

Fig. 8. W and σ_x Diagram ($l=100$ cm, $a=b=10$ cm, $t=t_0=2.5$ cm, $E=2.1\times10^5$ kg/cm^2, $\nu=0.15$).

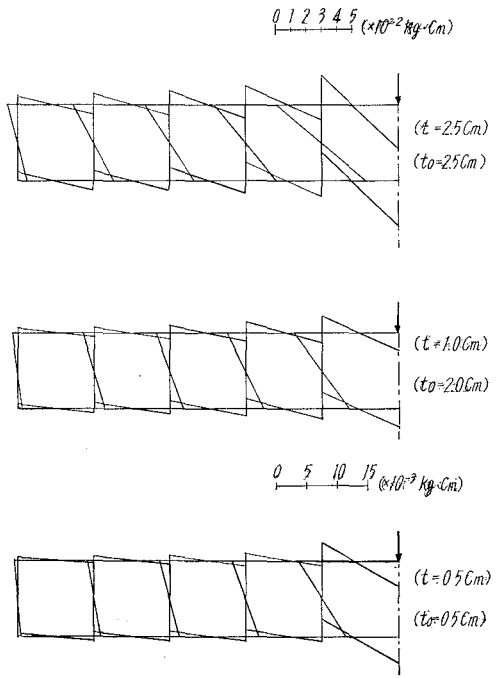

Fig. 9. Variation of Bending Moment in Midst profile.

repectively.

Fig. 9 illustrares the variation of the bending moments in the profile where $x=l/2$.

(b) In case of both free edge longitudinal joints subjected by equal concentrated loads,

$$P_0 = P_n = P \qquad \text{for} \quad x = f,$$
$$P_0 = P_n = 0 \qquad \text{for} \quad x = f,$$
$$P_r = 0,$$

from which

$$P_{0m} = P_{nm} = P \sin \frac{m\pi f}{l}.$$

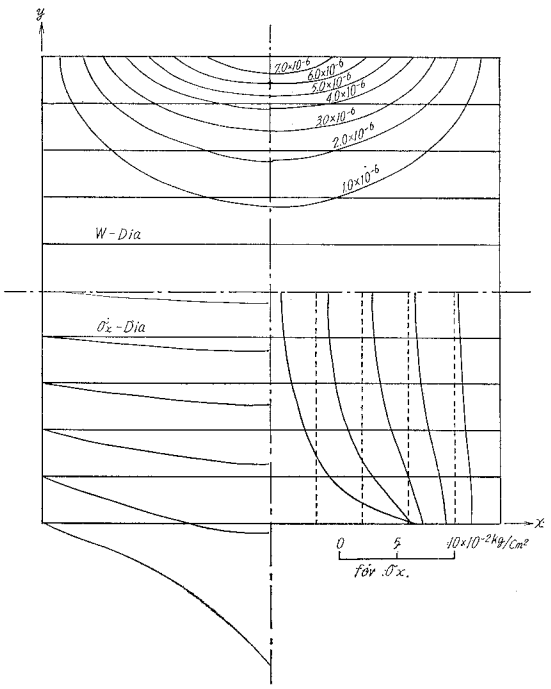

Fig. 10. w and σ_x Diagram ($l=100$ cm, $a=b=10$ cm, $t=t_0=0.5$ cm, $E=2.1\times10^6$ kg/cm, $\nu=0.3$).

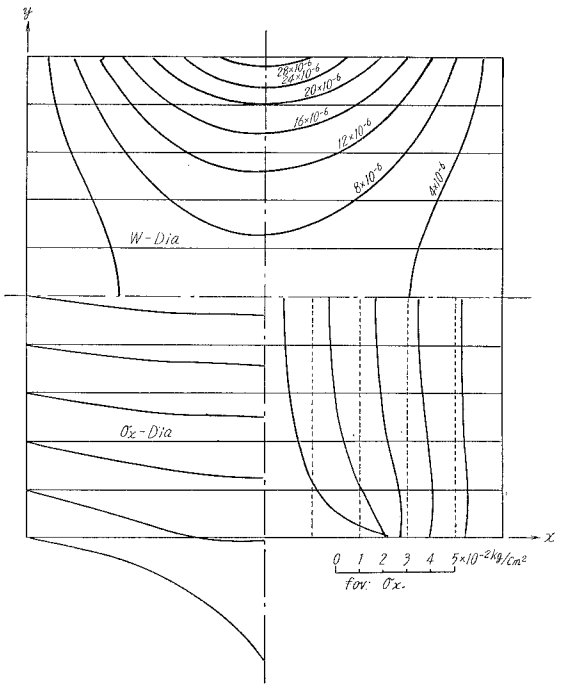

Fig. 11. w and σ_x Diagram ($l=100$ cm), $a=b=10$ cm, $t=1.0$ cm, $t_0=2.0$ cm, $E=2.1\times10^5$ kg/cm $\nu=0.15$).

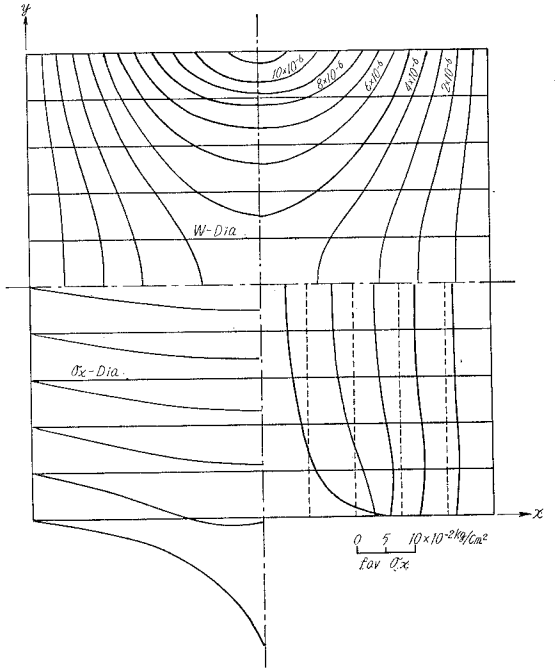

Fig. 12. w rnd σ_x Diagram ($l=100$ cm, $a=b=10$ cm, $t=t_0=2.$ cm, $E=2.1\times10^5$ kg/cm, $\nu=0.15$).

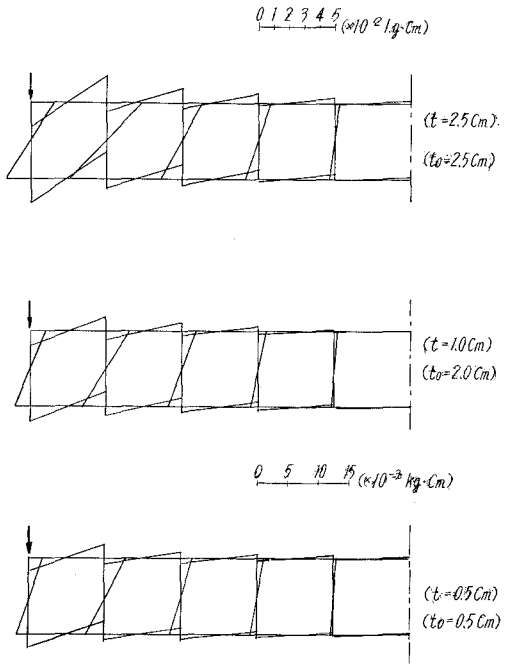

Fig. 13. Variation of Bending Moment in Midst Profil.

The diagrams of σ_x and w are shown in Fig. 10, 11, and 12 of which the coefficients are those of Fig. 6, 7, and 8, respectively. The variations of the bending moments in the midst profiles are as shown in Fig. 13. The computation was carryed on by FACOM 231 which is a midium size electric digital computor with 32000 bits. As for the calculation of infinite sine series, m was taken up to twenty; while the computation of σ_x and the joint bending moment at ten equidistant positions on every longitudinal joint, needed two hours and a half through the flow chart as follows:

FLOW CHART

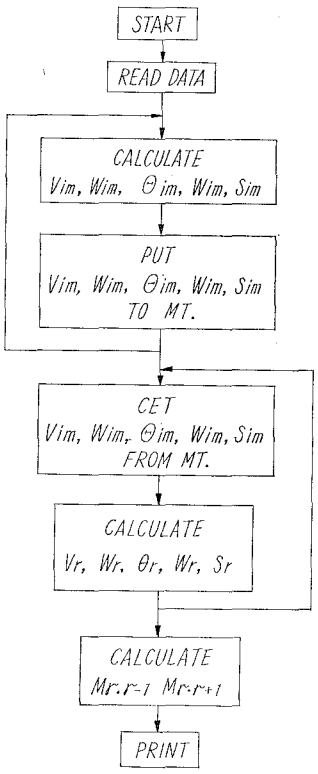

7. Closing Remark

The stiffness matrix for the prescribed numerical computation may be up to 30×30 one by means of the usual folded plate theory, whereas the method mentioned above needs only 3×3 matrix. Generally speaking, though there are some limitation for the layout of the component strips, the former method must treat m times calculations of 30×30 matrix and the later one has to deal with $m\times(n-1)$ 3×3 matrix. If we want to have the result for the structure of a similar shape with P', l', E', in stead of P, l, E; the corresponding result may be written in

$$w'=w\frac{P'El}{PE'l'}\,,\qquad \sigma_x'=\sigma_x\frac{P'l^2}{Pl'^2}\,.$$

in which the normal stress in the x direction at the r joint is as follows

$$\sigma_x=\frac{P_x}{t}=E\dot{u}_r+\nu S_r/t=E\ddot{w}_r+\nu S_r/t\,.$$

References

1) Jaeger, K.: Stahlbeton-Brückentrager mit mehrzelligem Kastenquerschnitt, Osterreichische Bauzeitschrift, 11 1956, S. 17.
2) Little, G., Rowe, R. E.: Load Distributions in Multiwebbed Bridge Structures from Plastic Models, Magazin of Concrete Research, Nov., (1955).
3) Naruoka, M., I. K., S. S.: AN EXPERIMENTAL STUDY ON MULTICELL STRUCTURES, TRANS. J. S. C. E. No. 87 (1962) p. 1.
4) Goldberg, J. E. Leve, H. L.: Theory of Prismatic Folded Plate Structures, IABSE, Zurich, Switzerland, No. 87, p. 71.
5) DeFries-Skene, A., Scordelis, A. C.: DIRECT STIFFNESS SOLUTION FOR FOLDED PLATES, Jourmal of Structural Division, ASCE, Aug. (1964), No. ST 4.
6) Chu, K., Pinjarkar, S.: MULTIPLE FOLDED PLATE STRUCTURES, Journal of Structural Division, ASCE, April (1966), ST 2.
7) Nomachi, S. G.: A Note on Finite Fourier Transforms Concerning Finite Integration, the Memoir of Muroran Inst. of Tech., **5**, 2 (1966), pp. 205–212.
8) Nomachi, S. G.: On a Method of Solving Grid Structure by Means of Fourier Transforms Concerning Finite Integration, the Memoirof Muroran Inst. of Tech., **6**, 1 (1967), pp. 91–100.